

Pauli-blocking Effect in a Quark Model

Sachiko Takeuchi

Japan College of Social Work, Kiyose, Japan

Kiyotaka Shimizu

Department of Physics, Sophia University, Chiyoda-ku, Tokyo, Japan

(Dated: December 4, 2018)

Pauli-Blocking effect on the kinetic term is investigated by employing the quark cluster model. The effect can be understood by the change of the degrees of the mixing between the incoming wave and the 0ℓ state of the inter-cluster wave function, which can be expressed by a potential which is highly nonlocal. We look into the properties of this effect by comparing equivalent local potentials. In the channel where the Pauli-blocking effect is small, the on-shell equivalent local potential simulates the nonlocal potential well even for the off-shell behavior. On the other hand, the off-shell behavior is very different from the original one where the effect is large. This off-shell behavior, however, can well be simulated by considering the nonlocal matrix elements only between the $0s$ state and the other states. The energy dependent potentials are also constructed and found to be helpful to understand the energy dependence of the effect.

PACS numbers: 12.39.Jh, 13.75.Ev, 03.65.Nk, 02.30.Zz 21.60.Gx,

Keywords: Pauli-blocking, Constituent quark cluster model, Inverse scattering, Equivalent local potential

I. INTRODUCTION

The cluster structure can often be seen in many-body systems. One of the famous examples is ${}^8\text{Be}$, where the ${}^4\text{He}$ structure has an important role [1]. It is also known, that the quark cluster model, where the baryon is considered as a cluster of three valence quarks, reproduces successfully many of the features of the two-baryon systems [2, 3, 4, 5, 6]. In this work, we focus our attention on the Pauli-Blocking effect on the kinetic term. We take the quark cluster model as an example though the definition, the procedure, and the basic feature discussed here can be applied to other cluster systems.

The Pauli-Blocking effect on the kinetic term should always be taken into account regardless of the interaction between the constituent fermions. In this sense, this can be considered as a ‘pure’ Pauli-Blocking effect on a concerning system. Actually, as was reported in ref. [7], in the channel where the Pauli-blocking effect plays an important role, the effect can still be seen in the phase shifts after the quark interactions are introduced.

The low-energy properties of the quark Pauli-blocking effect has been considered to cause a strong repulsion between two baryons in certain channels. It, however, also produces an attractive force for a higher energy region as we will discuss in detail in this paper. The Pauli-blocking effect among three or more clusters may become important [8]. Here, however, we concentrate on the two-cluster systems.

In this paper, we investigate the Pauli-blocking effect by constructing a nonlocal potential and by looking into the phase shifts and the wave functions of the systems with this potential. Then, we further investigate its properties by comparing four kinds of local potentials: 1) the one which gives the same scattering phase shift as that of the original nonlocal potential, 2) the one which gives the

same Born phase shift, 3) the energy-dependent potential obtained from the wave function, and 4) the energy-dependent potential obtained by using the WKB method.

The contents of this article is as follows. In section II, we define the nonlocal potential which expresses the Pauli-blocking effect on the nonrelativistic kinetic term. For this purpose, we employ the quark cluster model without any interaction between quarks. We will show that the effect can be taken into account by introducing a nonlocal two-baryon potential which does not depend on the energy.

In section III, we explain local potentials which express a part of the features of the nonlocal potential. In section III A, we mention that one can construct a unique potential which has the same on-shell behavior as that of a given nonlocal potential. In section III B, we construct a local potential which reproduces the same Born phase shift as that of the nonlocal potential. For this local potential, the analytic form can be obtained. In the next two subsections, two kinds of the energy-dependent local potentials are discussed. We mention that a potential can be obtained by a simple division by the wave function in section III C. The energy-dependent potential can also be derived with the help the WKB method, which is discussed in section III D.

The results are shown in section IV. In section IV A, we show that the Pauli-Blocking effect can be expressed in terms of a nonlocal potential, which is separable-like. It is found that the effect does not cause a simple attraction or repulsion. The phase shift changes its sign at the energy which corresponds to the kinetic energy of the relative 0ℓ state. As seen in section IV B, the local potential which gives the same on-shell behavior in the strongly prohibited channel is found to have a deep attractive pocket at the very short range. In the channel where the Pauli-blocking effect is small, or in the higher

partial-wave channels, this equivalent-local potential approach seems valid even for the off-shell behavior; the wave function is also similar to that of the original non-local potential. We find that the nonlocal treatment of the $0s$ - $1s$ component is essential to reproduce the off-shell behavior in the strongly prohibited channel, which is discussed in section IV C.

In section IV D, the energy dependence of the potentials is investigated. The energy-dependent potentials obtained by the division by the wave function have singularities at the node points of the wave function. They, however, are helpful to understand the energy dependence of the short range region. The energy dependent potentials given by the WKB method changes considerably as the energy increases. The potential barrier in the strongly prohibited channel disappears above a certain energy. At the very high energy, all the potentials become gradually smaller.

Summary is given in section V.

II. NONLOCAL POTENTIAL ARISING FROM PAULI-BLOCKING EFFECT

The nonlocal potential arising from Pauli-blocking effect can be obtained as follows. The Schrödinger equation for the constituent fermions (in the present problem, quarks) is

$$(H_q - E)\Psi = 0 \quad (1)$$

$$\left\{ \frac{H(\mathbf{r}, \mathbf{r}')}{N(\mathbf{r}, \mathbf{r}')} \right\} = \int d\boldsymbol{\xi}_A d\boldsymbol{\xi}_B d\mathbf{r}_{AB} \phi_A^\dagger(b, \boldsymbol{\xi}_A) \phi_B^\dagger(b, \boldsymbol{\xi}_B) \delta(\mathbf{r} - \mathbf{r}_{AB}) \left\{ \frac{H}{1} \right\} \mathcal{A}[\phi_A(b, \boldsymbol{\xi}_A) \phi_B(b, \boldsymbol{\xi}_B) \delta(\mathbf{r}' - \mathbf{r}_{AB})] . \quad (5)$$

This equation can be rewritten in the Schrödinger form as

$$\int \{ \overline{H}(\mathbf{r}, \mathbf{r}') - E \} \overline{\chi}(\mathbf{r}') d^3 \mathbf{r}' = 0. \quad (6)$$

The new kernel \overline{H} and the wave function $\overline{\chi}$ are defined as

$$\overline{H} = N^{-1/2} H N^{-1/2} \quad (7)$$

$$\overline{\chi} = N^{1/2} \chi. \quad (8)$$

The potential for baryons is defined from the above kernel as:

$$V_{QCM} = \overline{H} - K_D. \quad (9)$$

where K_D is the usual kinetic term of the two baryons with the mass $\sum m_i$. The Schrödinger equation with this potential,

$$(K_D + V_{QCM} - E)\psi = 0, \quad (10)$$

$$H_q = \sum_i \left(m_i + \frac{\mathbf{p}_i^2}{2m_i} \right) - \frac{\mathbf{p}_G^2}{2m_G} + V_q, \quad (2)$$

where m_i and \mathbf{p}_i are the mass and three momentum of the i th quark, respectively. In the quark cluster model, the wave function is assumed to have the following form [2, 3, 4, 5, 6]:

$$\Psi = \mathcal{A}_q \{ [\phi_\alpha(b, \boldsymbol{\xi}_A) \phi_{\alpha'}(b, \boldsymbol{\xi}_B)] \chi(\mathbf{r}_{AB}) \} \quad (3)$$

where \mathcal{A}_q is the antisymmetrization operator on the six quarks, $\phi_\alpha(b, \boldsymbol{\xi})$ is the single baryon wave function with the quantum number α , whose orbital part is the gaussian function with the size parameter b . By integrating the internal degrees of freedom out, we have the RGM (resonating group method) equation:

$$\int \{ H(\mathbf{r}, \mathbf{r}') - EN(\mathbf{r}, \mathbf{r}') \} \chi(\mathbf{r}') d^3 \mathbf{r}' = 0. \quad (4)$$

where H and N are the Hamiltonian and normalization kernels:

can be treated as the one for the baryon system with implicit internal degrees of freedom[7]. There are other definitions to extract a two-baryon potential from the RGM equation. For example, $V \equiv H - EN - (K_D - E)$ can be also taken as a potential between baryons. It, however, depends on the energy rather strongly while the nonlocality is still as large as the present one [9, 10]. The present definition is a unique way to remove the energy dependence from the two-baryon potential.

Suppose all of the particles cannot occupy the same orbital state at the same time because of the Pauli principle, the relative $0s$ two-cluster state is forbidden. When the system has such forbidden state(s), eqs. (7) and (8) are modified as

$$\overline{H} = (PNP)^{-1/2} (PHP) (PNP)^{-1/2} \quad (11)$$

$$\overline{\chi} = (PNP)^{1/2} P \chi \quad (12)$$

where, P is the projection operator on the space of all allowed states. The solution of the Schrödinger equation

eq. (10) should be orthogonal to the forbidden states. Since eigenvalues of both of the H and N become zero for the forbidden states, eqs. (11) and (12) can be defined as a natural extension of eqs. (7) and (8) as we will see later.

When we take only the nonrelativistic kinetic term as H_q , with no interaction between quarks, the hamiltonian kernel in eq. (4) can be replaced by the kinetic kernel, $K(\mathbf{r}, \mathbf{r}')$. Then, the QCM potential becomes,

$$V_K = N^{-1/2} K N^{-1/2} - K_D, \quad (13)$$

which is considered to express the effect of the Pauli-blocking on the kinetic term.

In this paper, we focus our attention on the single channel which has no forbidden state but the normalization kernel deviated from 1. Also, we take the two-cluster system where each cluster has three fermions with a common value for the mass, m_q . In this case, we only have one exchange term, provided that the relative wave function as well as the internal wave function of the clusters are antisymmetrized.

The normalization kernel $N(\mathbf{r}, \mathbf{r}')$ and the kinetic kernel $K(\mathbf{r}, \mathbf{r}')$ in eq. (4) become

$$N(\mathbf{r}, \mathbf{r}') = \delta(\mathbf{r} - \mathbf{r}') + N_{\text{ex}}(\mathbf{r}, \mathbf{r}') \quad (14)$$

and

$$K(\mathbf{r}, \mathbf{r}') = K_D + K_0 \left(\frac{15}{2} - \frac{27}{16b^2}(r^2 + r'^2) + \frac{21}{8b^2} \mathbf{r} \cdot \mathbf{r}' \right) N_{\text{ex}}(\mathbf{r}, \mathbf{r}') \quad (15)$$

respectively, where K_D is now the kinetic energy of the two-baryon system with the reduced mass $3m_q/2$, and $K_0 = 3/(4m_q b^2)$. The exchange part of the normalization kernel is obtained as

$$N_{\text{ex}}(\mathbf{r}, \mathbf{r}') = (\nu - 1) \left(\frac{27}{16\pi b^2} \right)^{\frac{3}{2}} \exp \left[-\frac{15}{16b^2}(r^2 + r'^2) + \frac{9}{8b^2} \mathbf{r} \cdot \mathbf{r}' \right]. \quad (16)$$

(See appendix.) The factor $(\nu - 1)$ is the matrix element of the exchange operator in the color-spin-flavor space, $-\langle \sum P_{ij} \rangle$. In our treatment here the model also includes the spectroscopic factor, which comes essentially from the difference in the number of combinations for picking up a cluster (three quarks out of six instead of one baryon out of two). Thus, the value of ν can be more than 1; actually, it is 0 or 10 when the states are totally antisymmetrized. In the following calculation, we take $\nu = 10/9$ or $2/9$ as an example, which are typical values for the single channel two-baryon systems.

Both of N and K can be expanded by the harmonic oscillator wave function with the size parameter $\beta = \sqrt{\frac{2}{3}}b$ as:

$$N(\mathbf{r}, \mathbf{r}') = \sum_{n\ell m} (1 + (\nu - 1) \theta^{2n+\ell}) \psi_{n\ell m}(\beta, \mathbf{r}) \psi_{n\ell m}^*(\beta, \mathbf{r}') \quad (17)$$

and

$$K(\mathbf{r}, \mathbf{r}') = \sum_{nn'\ell m} \frac{2K_0}{3} \left\{ \delta_{nn'} \left(2n + \ell + \frac{3}{2} \right) (1 + (\nu - 1) \theta^{2n+\ell}) \right. \\ \left. + (\delta_{nn'+1} + \delta_{nn'-1}) \sqrt{(n_{<} + 1) \left(n_{<} + \ell + \frac{3}{2} \right)} (1 + (\nu - 1) \theta^{2n_{<}+\ell}) \right\} \psi_{n\ell m}(\beta, \mathbf{r}) \psi_{n'\ell m}^*(\beta, \mathbf{r}') \quad (18)$$

where $\theta = 1/3$, $\psi_{n\ell m}$ is the harmonic oscillator wave function of the quantum number $n\ell m$, and $n_{<}$ corresponds to the smaller one among n and n' .

Thus the obtained V_K can be expressed as

$$V_K(\mathbf{r}, \mathbf{r}') = \sum_{nn'\ell m} V_K^{nn'\ell} \psi_{n\ell m}(\beta, \mathbf{r}) \psi_{n'\ell m}^*(\beta, \mathbf{r}') \quad (19)$$

with

$$V_K^{nn'\ell} = (\delta_{nn'+1} + \delta_{nn'-1}) \frac{2K_0}{3} \sqrt{(n_{<} + 1) \left(n_{<} + \ell + \frac{3}{2} \right)} \left\{ \sqrt{\frac{1 + (\nu - 1) \theta^{2n_{<}+\ell}}{1 + (\nu - 1) \theta^{2n_{<}+\ell+2}}} - 1 \right\} \quad (20)$$

As was mentioned before, eq. (20) is also valid even when $\nu = 0$, namely, a forbidden state exists, or when the

system contains the coupled channels.

Note that the diagonal part, namely, the $n = n'$ term, does not exist in V_K . The diagonal parts in the original $K(\mathbf{r}, \mathbf{r}')$ kernel are canceled out when K is divided by N and subtracted by K_D .

For the partial wave decomposition of the nonlocal potential below, we use the notation:

$$V_K(\mathbf{r}, \mathbf{r}') = \sum_{\ell m} V_{K\ell}(r, r') Y_{\ell m}(\mathbf{r}) Y_{\ell m}^*(\mathbf{r}'). \quad (21)$$

Since the terms in eq. (19) are of order $O((1/9)^n)$, only the small n terms are important. The radial part of the lowest-order term of eq. (20), where n or n' is zero, is written as

$$V_{K\ell}^{(0)}(r, r') = (\sqrt{\nu} - 1) \frac{2K_\beta}{3} \sqrt{\ell + \frac{3}{2}} \times (u_{0\ell}(\beta, r) u_{1\ell}(\beta, r') + u_{1\ell}(\beta, r) u_{0\ell}(\beta, r')) \quad (22)$$

where $u_{n\ell}$ is the orbital part of the harmonic oscillator wave function, $\psi_{n\ell m}$. From the above equation, it is clearly seen that the sign and magnitude of the potential changes according to those of $(\nu - 1)$.

Since r - and r' -dependence of the factor in eq. (22) is

$$u_{0\ell}(\beta, r) u_{1\ell}(\beta, r') + u_{1\ell}(\beta, r) u_{0\ell}(\beta, r') \propto \frac{2}{\beta^3} \left(\frac{rr'}{\beta^2} \right)^\ell \left(1 - \frac{1}{2\ell + 3} \frac{(r^2 + r'^2)}{\beta^2} \right) \times \exp\left[-\frac{(r^2 + r'^2)}{2\beta^2}\right], \quad (23)$$

the potential given by the lowest term has a rather simple structure.

For each of the angular momentum ℓ , the phase shift given by $V_{K\ell}$ with the Born approximation can be written as:

$$\begin{aligned} \tan \delta_\ell^{Born}(k) &= -2\mu k \int j_\ell(kr) V_{K\ell}(r, r') j_\ell(kr') r^2 dr r'^2 dr' \\ &= -2\mu k \sum_{nn'} V_K^{nn'\ell} \tilde{u}_{n\ell}(\beta, k) \tilde{u}_{n'\ell}(\beta, k) \end{aligned} \quad (24)$$

with $k^2 = 2\mu E$. The function $\tilde{u}_{n\ell}(\beta, k)$ is the Fourier transformation of the $u_{n\ell}(\beta, r)$, namely, $\tilde{u}_{n\ell}(\beta, k) = \sqrt{\pi/2} (-1)^n u_{n\ell}(1/\beta, k)$.

The momentum which gives $\delta(k_0) = 0$, k_0 , can be obtained as the solution of $\tilde{u}_{n=1\ell}(\beta, k_0) = 0$ approximately. This momentum k_0 depends on the cluster size parameter, b , but does not depend on ν nor other parameters. When $0 < \nu \ll 1$, the resonance becomes sharper, but the resonance momentum does not change. The resonance energy of the almost-forbidden channel is given by $\beta^2 k_0^2 \sim (\ell + \frac{3}{2})$, which corresponds to the kinetic energy of the 0ℓ state.

III. LOCAL POTENTIALS

A. On-shell-equivalent local potential

A local potential can be constructed uniquely from a given S -matrix, $S(k)$, by using the Marchenko-method[7, 11, 12, 13]. The procedure is as follows. First, the following function $F(r)$ should be calculated from the S -matrix with poles at $\{k = i\kappa_j\}$,

$$F(r) = -\frac{1}{2\pi} \int_{-\infty}^{+\infty} e^{ikr} \{S(k) - 1\} dk + \sum_j c_j^2 e^{-\kappa_j r}, \quad (25)$$

where c_j^2 is

$$c_j^2 = \text{Residue}\{S(k)\} \text{ at } k = i\kappa_j \ (\kappa_i > 0). \quad (26)$$

Next, we solve the following integral equation with $F(r)$.

$$K(r, r') = -F(r + r') - \int_r^\infty F(r + r'') K(r, r'') dr''. \quad (27)$$

Then, the local potential $V(r)$ is obtained from the solution of the above equation, K , as

$$2\mu V(r) = -2 \frac{d}{dr} K(r, r), \quad (28)$$

where μ is the reduced mass of the system. The more detailed calculation is found, for example, in ref. [7].

We construct a local potential from the phase shift given by the nonlocal potential V_K . The obtained potential is the momentum- and energy-independent, but depends on the angular momentum ℓ . We call this the on-shell-equivalent local potential from now on. Its on-shell behavior, namely the asymptotic behavior of the wave function obtained by solving the Schrödinger equation with that potential, is the same as that of the original nonlocal potential. The off-shell feature, however, can be very different from the original one when the degree of the nonlocality is large. The difference can be seen, for example, by looking into the wave functions at finite r .

For the system with a forbidden state, one can also construct a potential which reproduces the phase shift. When the wave function of the forbidden state behaves asymptotically for large r as $\exp[-ar]$, the on-shell-equivalent local potential is also uniquely constructed from its binding energy and residue together with the phase shifts. The wave functions obtained by solving this local potential, however, are not orthogonal to the original wave function of the forbidden state in general. Moreover, in the present problem, the forbidden state is bounded by the confinement force. A local potential with a finite size cannot produce the asymptotic behavior of its wave function, $\exp[-ar^2]$.

As we will show later, there are channels where the Pauli-blocking effect is strong even though it does not produce a forbidden state. There, the off-shell behavior

of the on-shell-equivalent local potential is very different from the original one. For that case, we consider the partially local potential, where the $0s$ - $1s$ component is treated as nonlocal,

$$V^{0s\text{-nonloc}}(r, r') = V_{K\ell}^{(0)}(r, r') + V_{loc}^{0s\text{-nonloc}}(r) \frac{\delta(r - r')}{r^2}. \quad (29)$$

There may be no existence nor uniqueness for the local part, $V_{loc}^{0s\text{-nonloc}}$. In the case we will describe later, however, we can find $V_{loc}^{0s\text{-nonloc}}$ by fitting the phase shifts.

B. Born-Equivalent local potential

It is also useful to look into the local potential which can be expressed in an analytic form. For a system with no bound state nor the forbidden state, we construct the local potential which reproduces the same Born phase shift as that of the nonlocal potential. We call this Born-equivalent local potential.

The Born-equivalent local potential is the same as the on-shell-equivalent local potential when the original potential is local, even where the Born approximation is not valid. It, however, deviates from the on-shell-equivalent potential in general when the original potential is nonlocal. Thus, we consider the size of the deviation as a rough estimate of the size of the nonlocality.

Suppose the system does not have a bound state. Then, the phase shift by the first Born approximation, which is the Fourier transformation of the potential, contains enough information to construct a local potential. For example, it is obtained uniquely for $\ell = 0$ by the cosine Fourier transformation. From the known $\delta_{\ell=0}^{Born}(k)$,

$$\tan \delta_{\ell=0}^{Born}(k) = -2\mu k \int j_0(kr) V_{\ell=0}(r) j_0(kr) r^2 dr \quad (30)$$

$$= \frac{\mu}{k} \left(\int_0^\infty \cos(2kr) V_{\ell=0}(r) dr + const. \right), \quad (31)$$

$V_{\ell=0}(r)$ is obtained as

$$V_{\ell=0}(r) = \frac{4}{\pi} \int_0^\infty \frac{k}{\mu} \tan \delta_{\ell=0}^{Born}(k) \cos(2kr) dk \quad (32)$$

with an ambiguity of the Dirac's delta function at $r = 0$, which does not contribute to the observables.

The explicit form for the $\ell = 0$ system of the present issue, for example, can be obtained as

$$V_{\ell=0}(r) = -\frac{8}{\pi} \sum_{\substack{nn' \\ \ell=m=0}} V_K^{nn'\ell} \times \int_0^\infty \tilde{u}_{n\ell}(k) \tilde{u}_{n'\ell}(k) \cos(2kr) k^2 dk. \quad (33)$$

The one which corresponds to $V_{K\ell=0}^{(0)}$ in eq. (22) is:

$$V_{K0}^{(0) \text{ Born}} = 16K_0 (\sqrt{\nu} - 1) \frac{r^2}{\beta^2} \left(1 - \frac{2}{3} \frac{r^2}{\beta^2} \right) \exp\left[-\frac{r^2}{\beta^2}\right]. \quad (34)$$

The sign of this potential changes at $r \sim \sqrt{\frac{3}{2}}\beta = b$.

C. Energy-dependent local potential (by direct division)

An energy-dependent potential can be obtained directly by dividing the hamiltonian by the obtained wave function. When $\psi(r)$ is a solution of the Schrödinger equation with a local potential $V(r)$, $V(r)$ can be reconstructed from the wave function:

$$V(r) = E - \frac{1}{2\mu} \frac{p^2 \psi(r)}{\psi(r)} \quad (35)$$

Suppose ψ is the solution of the Schrödinger equation with a nonlocal potential, $V(r)$ obtained from the above equation can also be considered as an equivalent local potential, which depends on all of ℓ , r , and E .

The potential obtained this way gives the same phase shift and the wave function as the original nonlocal potential. The potential, however, may have a singularity of the order $1/(r - r_0)$ at the node points of the wave function in general. Nevertheless, we discuss this potential to show the energy dependence of the Pauli-blocking effect. It has an advantage that one can always construct this potential except the node point of the wave function unlike the one defined using WKB in the next subsection.

D. Energy-dependent local potential (by WKB method)

One of the conventional ways to treat the nonlocality of the potential is to interpret it as the energy dependence by using the WKB method [14].

In this subsection, we explain the effect of the nonlocality and a relation between the nonlocality and energy dependence. The nonlocal part has the following form in the Schrödinger equation.

$$\int \langle \mathbf{r} | V | \mathbf{r}' \rangle \chi_\ell(\mathbf{r}') d\mathbf{r}' \quad (36)$$

Introducing $\mathbf{s} = \mathbf{r}' - \mathbf{r}$, we obtain

$$\begin{aligned} & \int \langle \mathbf{r} | V | \mathbf{r}' \rangle \chi_\ell(\mathbf{r}') d\mathbf{r}' \\ &= \int \exp\left(\frac{\nabla \cdot \mathbf{s}}{2}\right) U(\mathbf{r}, \mathbf{s}) \exp\left(\frac{\nabla \cdot \mathbf{s}}{2}\right) d\mathbf{s} \chi_\ell(\mathbf{r}) \end{aligned} \quad (37)$$

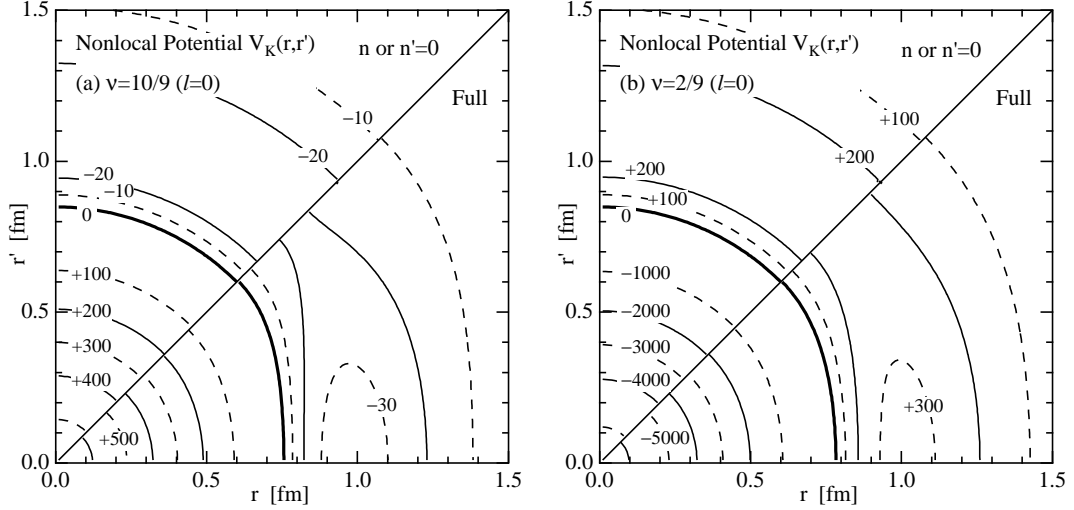


FIG. 1: Contour plot of the original nonlocal potential $V_{K\ell}(r, r')$ for the $\ell = 0$ channel. (a) is for the $\nu = 10/9$ case, and (b) is for the $\nu = 2/9$ case. In the upper half of each figure we plot the lowest-order term (n or $n' = 0$), defined in eq. (22).

Here we have used the following relations:

$$\chi_\ell(\mathbf{r}') = \chi_\ell(\mathbf{r} + \mathbf{s}) = \exp(\nabla \cdot \mathbf{s}) \chi_\ell(\mathbf{r}) \quad (38)$$

and

$$\begin{aligned} \langle \mathbf{r} | V | \mathbf{r}' \rangle &= U\left(\frac{\mathbf{r} + \mathbf{r}'}{2}, \mathbf{s}\right) = U\left(\mathbf{r} + \frac{\mathbf{s}}{2}, \mathbf{s}\right) \\ &= \exp\left(\frac{\nabla \cdot \mathbf{s}}{2}\right) U(\mathbf{r}, \mathbf{s}) \exp\left(-\frac{\nabla \cdot \mathbf{s}}{2}\right) \end{aligned} \quad (39)$$

Assuming that $U(\mathbf{r}, \mathbf{s})$ does not change rapidly within a distance s , we get a momentum dependent local potential

$$\begin{aligned} &\int \langle \mathbf{r} | V | \mathbf{r}' \rangle \chi_\ell(\mathbf{r}') d\mathbf{r}' \\ &= \int U(\mathbf{r}, \mathbf{s}) \exp(\nabla \cdot \mathbf{s}) d\mathbf{s} \chi_\ell(\mathbf{r}) = U(\mathbf{r}, \mathbf{p}) \chi_\ell(\mathbf{r}). \end{aligned} \quad (40)$$

Here ∇ acts only on the wave function and thus replaced by the momentum operator \mathbf{p} . The present potential is central and depends on \mathbf{p} and \mathbf{r} only through p^2 , r^2 and $(\mathbf{p} \cdot \mathbf{r})^2$. By substituting $(\mathbf{p} \cdot \mathbf{r})^2 \rightarrow p^2 r^2 - (\ell + 1/2)^2$, we have the potential, $U(r, p)$, which depends only on p^2 and r^2 .

Employing the classical approximation,

$$\frac{p^2}{2\mu} + U(r, p) = E \left(= \frac{k^2}{2\mu} \right) \quad (41)$$

we obtain the energy-dependent local potential, $U(r, E)$ by solving eq. (41) for each r and E with the explicit form of $U(r, E)$.

For the n or $n' = 0$ term of the $\ell = 0$ channel, we find that $U(r, p)$ has the form,

$$\begin{aligned} U_{\ell=0}^{(0)}(r, p) &= (\sqrt{\nu} - 1) \frac{32}{3} K_\beta \left(-\frac{r^2}{\beta^2} + \beta^2 p^2 \right) \\ &\times \exp[-\beta^2 p^2] \exp\left[-\frac{r^2}{\beta^2}\right]. \end{aligned} \quad (42)$$

When $\beta^2 p^2$ is small, the potential becomes

$$\begin{aligned} U_{\ell=0}^{(0)}(r, E) &\sim \\ &\frac{8(\sqrt{\nu} - 1)}{\mu\beta^2} \frac{\left\{ -\frac{r^2}{\beta^2} + 2E\mu\beta^2 \left(1 + \frac{r^2}{\beta^2} \right) \right\} \exp\left[-\frac{r^2}{\beta^2}\right]}{1 + 16(\sqrt{\nu} - 1) \left(1 + \frac{r^2}{\beta^2} \right) \exp\left[-\frac{r^2}{\beta^2}\right]}. \end{aligned} \quad (43)$$

For the $\nu > 1$ case, the potential is negative definite at $E = 0$ and increases as the energy increases. When U is small compared to E , then $U(r, E)$ decreases by the factor $\exp[-2\mu\beta^2 E]$.

IV. RESULTS

A. Nonlocal potential

The nonlocal potential, $V_K(r, r')$, defined by eq. (13) and its diagonal part, $V_K(r, r' = r)r^2$, are shown in Figure 1 (contour plot) and in Figure 2, respectively, for the $\ell = 0$ channel. The cluster size parameter here is $b = 0.6$ fm, and the quark mass is taken to be $m_q = 313$ MeV. In Figures 1(a) and 2(a), we plot the potential for the $\nu = 10/9$ case, which corresponds to the even partial wave of the NN channel. Overall size is small because

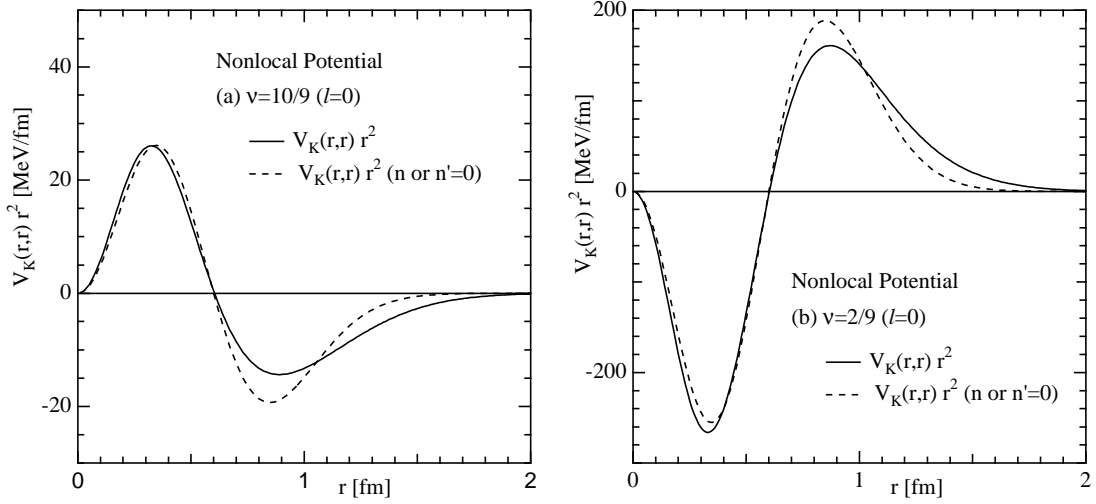


FIG. 2: Diagonal part of the original nonlocal potential, $V_{K\ell}(r, r')r^2$, for the $\ell = 0$ channel. The solid lines are for the full calculation, and the dotted lines are for the lowest-order term. (a) is for the $\nu = 10/9$ case, and (b) is for the $\nu = 2/9$ case.

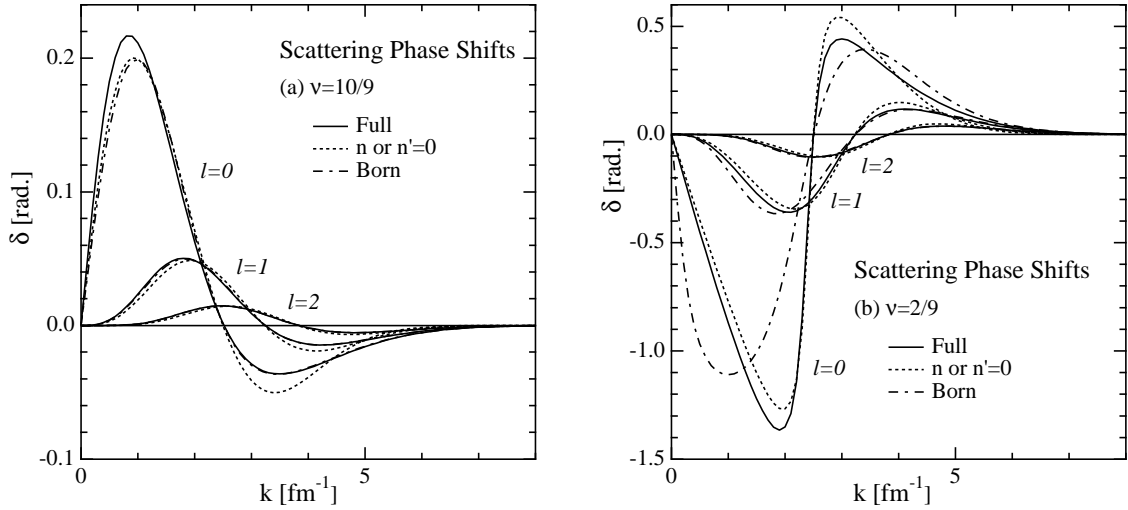


FIG. 3: Scattering phase shifts obtained from the original nonlocal potential $V_{K\ell}$ for the $\ell = 0, 1$ and 2 . The solid lines are for the full calculation, the dotted lines are for the lowest-order term, and the dot-dashed lines are the results from the Born approximation. (a) is for the $\nu = 10/9$ case, and (b) is for the $\nu = 2/9$ case.

ν is close to one. Figures 1(b) and 2(b) correspond to the $\Sigma N(I=3/2, S=1)$ channel, where the Pauli-blocking effect is strong ($\nu = 2/9$). There the size is very large; it is about $7/9$ times as large as the kinetic energy of the 0ℓ state in the short range region.

In the contour plots, we plot the potential given by the lowest term, $V_{K\ell}^{(0)}(r, r')$ in eq. (22), in the upper halves. The potential $V_{K\ell=0}^{(0)}$ depends only on $(r^2 + r'^2)$ for the $\ell = 0$ channel. The full potentials, written in the lower halves, however, have more complicated structure around $r \sim 1$ fm.

The scattering phase shift obtained from the nonlocal potential V_K is shown in Figure 3 in solid lines. For the $\nu = 10/9$ case (Figure 3(a)), the phase shift is positive at the low energy region. It, however, goes negative above about $\beta k \sim \sqrt{\ell + \frac{3}{2}}$, the momentum of the 0ℓ state. When ν becomes small, there appears an almost-forbidden resonance at this momentum. In the $\nu = 2/9$ system (Figure 3(b)), the phase shift is negative at the low-energy region while it becomes positive above a certain energy. The reason is as follows. The direct part of the kinetic energy mixes the $0s$ and $1s$ states; when

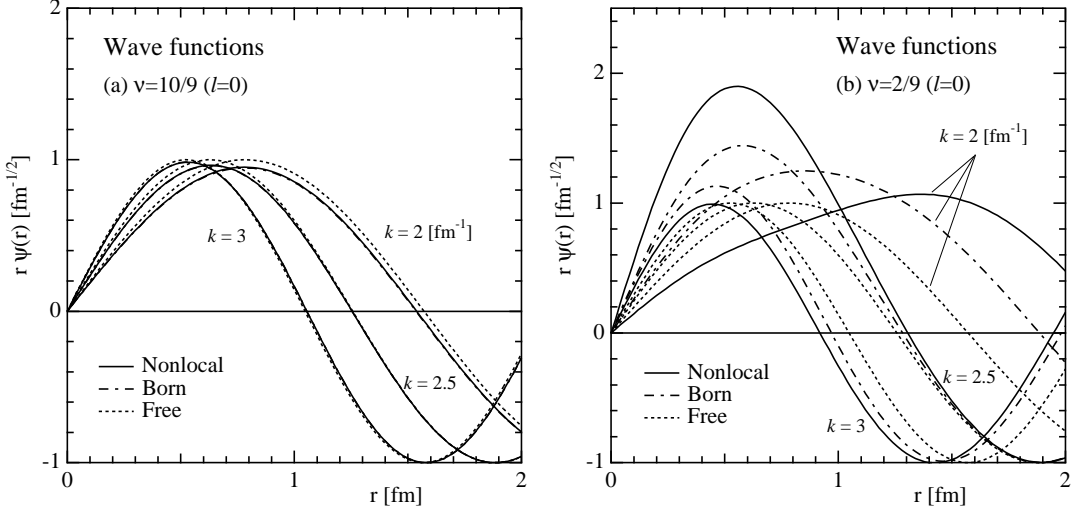


FIG. 4: Wave functions obtained from the original nonlocal potential $V_{K\ell}$ for the $\ell = 0$ channel. The dotted lines are the free wave function, and the dot-dashed lines are the results from the Born approximation. (a) is for the $\nu = 10/9$ case, and (b) is for the $\nu = 2/9$ case.

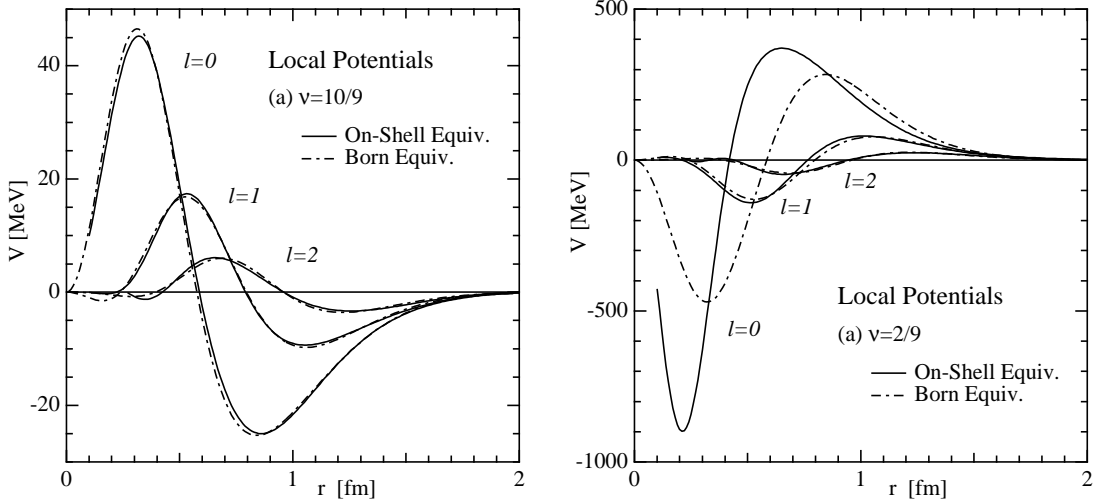


FIG. 5: On-shell-equivalent local potentials and Born-equivalent local potentials (see text). (a) is for the $\nu = 10/9$ case, and (b) is for the $\nu = 2/9$ case.

$\nu < 1$, this mixing is suppressed by the potential in eq. (22). Above the kinetic energy of the 0ℓ state, the potential becomes attractive, which also comes from the suppression of the mixing. On the other hand, when $\nu > 1$, the mixing is enhanced. Then, the potential becomes attractive in the low energy region and repulsive in the high energy region. The phase shift given by the lowest-order term, eq. (22), is also plotted in Figure 3 in dotted lines. The full phase shifts are well-approximated by the lowest-order term.

The Born phase shifts of the original nonlocal potential are plotted also in Figure 3 by dot-dashed lines.

The overall feature of the $\nu = 10/9$ channel is well reproduced by this approximation. Since the potential is stronger, the Born approximation does not work well in the $\nu = 2/9$ $\ell = 0$ channel. The momentum which gives $\delta(k_0) = 0$, k_0 , however, is well simulated. As we mentioned before, this momentum is obtained as the solution of $\phi_{n=1\ell}(k_0) = 0$ approximately. Here, $k_0 \sim \frac{3}{2b} = 2.5 \text{ fm}^{-1}$ for the $\ell = 0$ channel.

The wave functions obtained from this nonlocal potential as well as the ones from the Born-approximation are plotted in Figure 4 for higher momentum $k = 2, 2.5$,

and 3 fm^{-1} ($E = 166, 259$, and 373 MeV , respectively.) Those of the $\nu = 10/9$ $\ell = 0$ channel are shown in Figure 4(a); the wave functions are very close to the free wave functions for all k . On the other hand, the wave functions of the $\nu = 2/9$ $\ell = 0$ channel shown in Figure 4(b) deviate largely from the free wave function. At $k = 2.5 \text{ fm}^{-1}$, where the phase shift is almost zero, there is a large enhancement of the wave function at the short range region. This comes from the attraction at short distance of the nonlocal potential. This tendency can also be seen for the Born wave function. The degree of the enhancement, however, is different even where the Born phase shift is close to the original one; the original wave function is much larger than that of the Born approximation at $k = 2.5 \text{ fm}^{-1}$, whereas it becomes smaller at $k = 3 \text{ fm}^{-1}$. The energy dependence of the original wave function is much larger than the Born wave function.

B. Equivalent potentials

In Figure 5, we plot the on-shell-equivalent local potentials obtained for the $\nu = 10/9$ (Figure 5(a)) and $\nu = 2/9$ (Figure 5(b)) channels in solid lines. The potential for $\nu = 10/9$ is attractive at long range and repulsive at short range. Overall size, however, remains rather small. The potential for the $\nu = 2/9$ system has an opposite sign and is very large. Especially, the $\ell = 0$ system has an exceptional feature. It has large potential barrier at the longer distance with a deep attractive pocket in the short range. There is a quasi-bound state in this pocket; the scattering wave function is orthogonal approximately to the state except for around the resonance energy. To have such a pocket is the way to express an almost forbidden state by a local potential.

The wave functions obtained from the on-shell-equivalent local potential are plotted in Figures 6 and 7 for the $\ell = 0$ wave. It is found that the wave function is similar to the original one for the $\nu = 10/9$ case. On the other hand, the wave function of the system with an almost-forbidden state has an artificial bump at the short distance at the low energy.

The Born-equivalent local potentials are plotted also in Figure 5. They are similar to the on-shell-equivalent local potentials except for the $\nu = 2/9$ $\ell = 0$ channel. There, both of the barrier and the attractive pocket of the on-shell-equivalent potential are more manifest. As seen in Figure 3(b), Born approximation is not valid in this channel. Even so, the fact that those two potential deviate from each other indicates the nonlocality of the original potential. Though the size of the deviation is probably affected by the Born approximation, it seems safe to conclude that the nonlocality is very large in this channel.

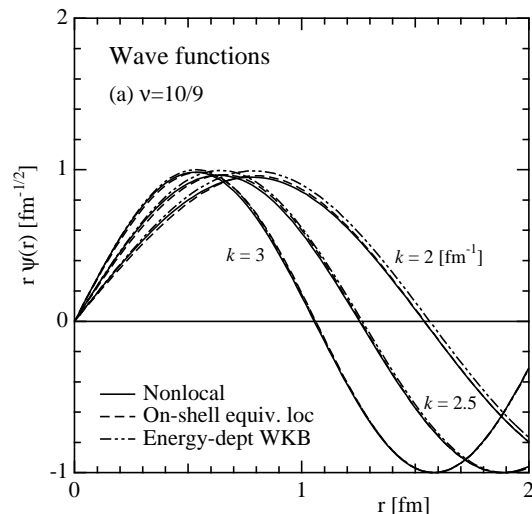


FIG. 6: Wave functions obtained from the on-shell equivalent local potential (dashed lines) and that from the original nonlocal potential (solid lines) for the $\nu = 10/9$ case. The result from the energy-dependent potential is also plotted by the double-dot-dashed line.

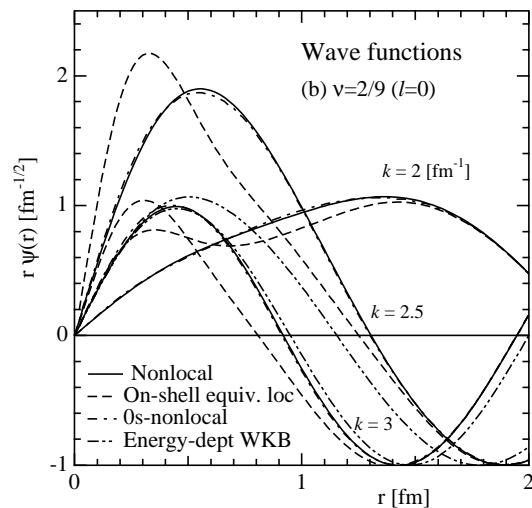


FIG. 7: Wave functions obtained from the on-shell equivalent local potential (dashed lines) and that from the original nonlocal potential (solid lines) for the $\nu = 2/9$ case. That from the partially local potential defined by eq. (29) (dot-dashed lines) and that from the energy-dependent potential (double-dot-dashed lines) are also plotted.

C. Partially local potential

We obtained the local part in the partially local potential, $V_{loc}^{os-nonloc}(r)$, defined by eq. (29) for the $\nu = 2/9$ $\ell = 0$ channel. The size of this local part becomes much smaller than the on-shell-equivalent local poten-

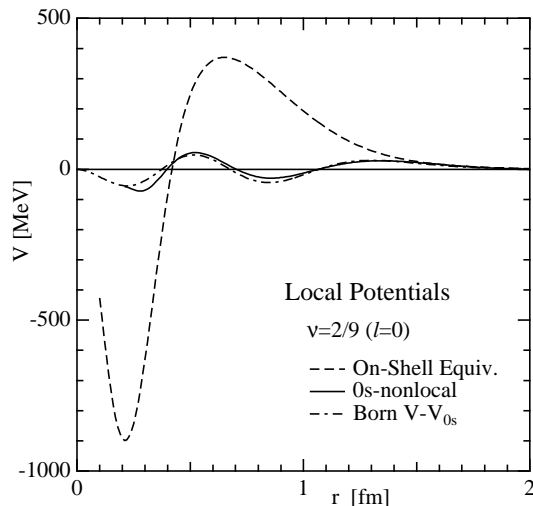


FIG. 8: Local part of the partially local potential, $V_{loc}^{0s-\text{nonloc}}(r)$, for the $\nu = 2/9$ case defined by eq. (29). The difference between the full and $0s$ - $1s$ part of the Born-equivalent local potential is also plotted in the dot-dashed line.

tial, and is found to have more nodes as seen in Figure 8. We also plot the higher-order term of the Born-equivalent potential, namely, the difference between the Born-equivalent potential of the full potential and that of the n or $n' = 0$ term. This higher-order term is very similar to $V_{loc}^{0s-\text{nonloc}}(r)$, while the on-shell equivalent potential is very different from the Born-equivalent one. This suggests that it is important to take the nonlocality in the n or $n' = 0$ term into account.

The wave function corresponding to this partially local potential is also shown in Figure 7. The obtained wave function is similar to that of the nonlocal potential. This confirms that the term between the $0s$ and the other states is the dominant part of the nonlocal potential and that the nonlocality can be taken care of by considering this term.

D. Energy-dependent potentials

The energy-dependent potentials constructed from the s -wave wave functions by eq. (35) are plotted in Figure 9. As we discussed in the previous section, there is a singularity at each of the node points of the wave function. Also, numerical error is large at $r \sim 0$. Nevertheless, one can see that, for the $\nu = 10/9$ channel, the short range part increases as the energy increases. As for the $\nu = 2/9$ channel, a large repulsive core appears at the low energy region, which decreases rapidly as the energy increases. Above $k \sim 2.5 \text{ fm}^{-1}$, the short range repulsion disappears.

The momentum-dependent potentials obtained by the

WKB method, $U(r, p)$ in eq. (41), are plotted in Figure 10. As seen from Figure 10(a), $U(r, p)$ of the $\nu = 10/9$ $\ell = 0$ channel is negative definite at $p = 0$. As the momentum increases, a repulsion appears at the short range region. $U(r, p)$ of the $\nu = 2/9$ $\ell = 0$ channel is shown in Figure 10(b), which is the same as the other channel except for the overall amplitude and sign.

For the $\nu = 10/9$ case, by solving eq. (41) self-consistently, we have the energy-dependent potentials, $U(r, E)$, which are shown in Figure 11(a). It shows similar behavior to the momentum-dependent potential. At $E = 0 \text{ MeV}$, or $k = 0 \text{ fm}^{-1}$, it is simply attractive. As the energy increases, however, the repulsive part appears at the short range. As discussed in eq. (43), when $\beta^2 p^2$ is small, the potential at $r = 0$ increases by $\frac{16(\sqrt{\nu}-1)}{1+16(\sqrt{\nu}-1)}E$, which is $0.46E$. Though one has to add the contribution from the interaction to see the energy dependence of the repulsive core of the two-baryon systems, it is interesting to see that the short-range part of the potential may move by a large amount as the energy increases. Above about $k = 3 \text{ fm}^{-1}$, the potential gradually decreases.

The phase shift given by this energy-dependent local potential from the WKB method is plotted in Figure 12(a). Overall feature is well simulated by this potential. The momentum where the sign of the phase shift changes, however, becomes smaller. The deviation from the original one comes from the approximation used to derive eq. (40) from eq. (39), but not from the WKB method. This is confirmed by employing the Born approximation for each potential in eq. (39) and in eq. (40), which is shown also in Figure 12.

We plot the wave function from the energy-dependent potential by WKB method for the $\nu = 10/9$ case in Figure 6. The wave function is similar to the original one in spite of the deviation found in the phase shift, probably because the size of the potential is rather small.

The $\nu = 2/9$ potential shows more notable feature. There are two real solutions to fill the conditions eq. (41) for each r and E at energy higher than $k = 2.5 \text{ fm}^{-1}$. On the other hand, at energy lower than $k = 2.5 \text{ fm}^{-1}$, the solutions have a complex value around $r \sim 0.7 \text{ fm}$.

In the Figure 11(b), we plot the solution which goes to zero at $r \rightarrow \infty$ for $k \geq 2.5 \text{ fm}^{-1}$. At $k = 2.5 \text{ fm}^{-1}$, the potential has attractive pocket in the short range region with a barrier around $r \sim 0.7 \text{ fm}$. Both of the barrier and the attractive pocket becomes smaller as the energy increases.

The phase shifts for $k \geq 2.5 \text{ fm}^{-1}$ of the $\nu = 2/9$ case are shown for in Figure 12(b). The resonance also moves to a smaller momentum. The deviation also seems to come from the approximation used to derive eq. (40) from eq. (39).

The wave function from the energy-dependent potential by WKB method for the $\nu = 2/9$ case in Figure 7. The wave function at $k = 3 \text{ fm}^{-1}$ is similar to the nonlocal one. On the other hand, that of $k = 2.5 \text{ fm}^{-1}$ deviates largely because the resonance occurs at the lower energy.

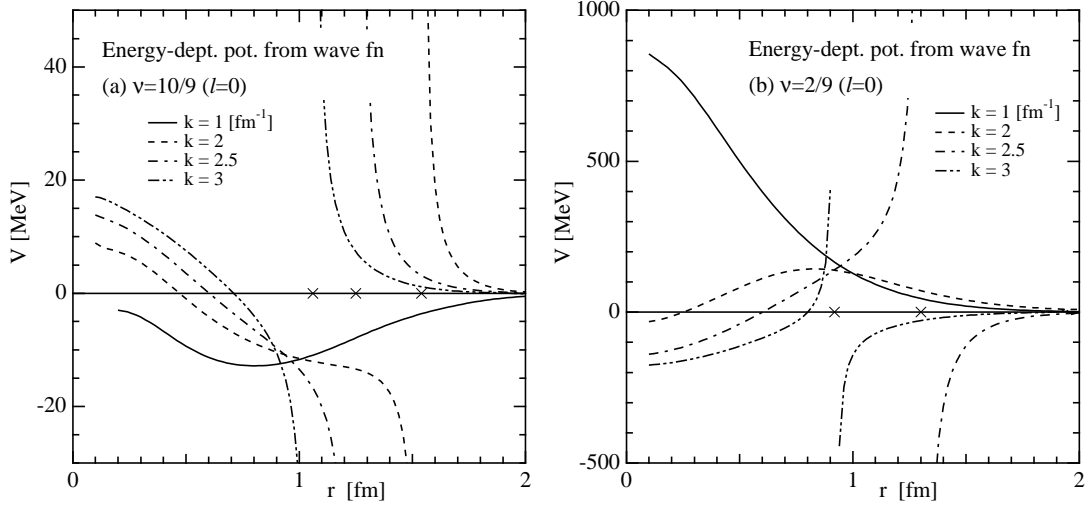


FIG. 9: Energy-dependent potentials by division (see text). (a) is for the $\nu = 10/9$ case, and (b) is for the $\nu = 2/9$ case. Node points of the wave functions are marked by \times 's.

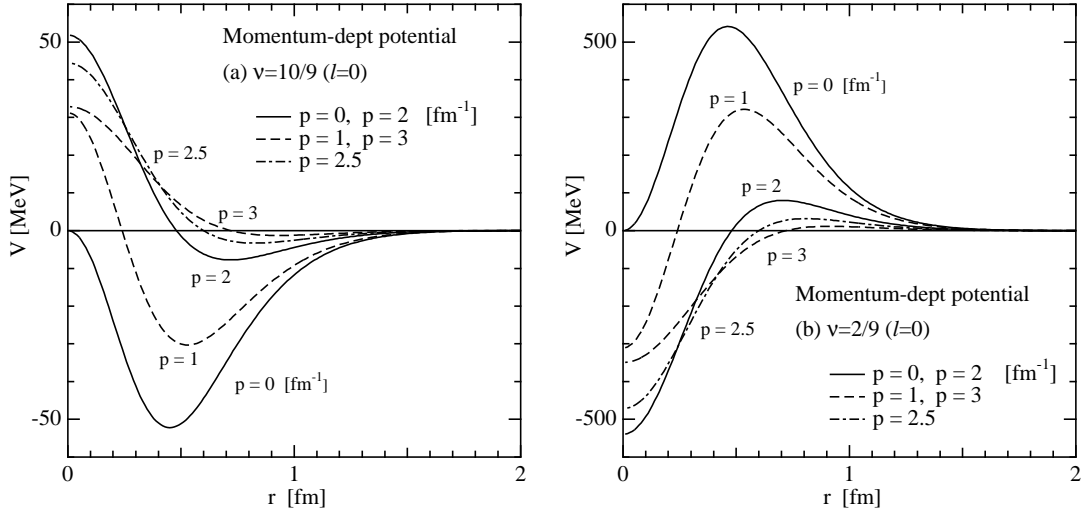


FIG. 10: Momentum-dependent potentials, $U(r, p)$ (see text). (a) is for the $\nu = 10/9$ case, and (b) is for the $\nu = 2/9$ case.

V. SUMMARY

Pauli-Blocking effect on the kinetic term is investigated by employing the quark cluster model. The effect can be expressed by a potential which is highly nonlocal. It is found that the Pauli-Blocking effect does not cause a simple attraction or repulsion. In order to see this point, we have calculated the phase shifts for two cases, namely, the one where the normalization factor ν (see eq. (16)) is larger than 1 and the other case where ν is smaller than 1. In the first case ($\nu = 10/9$, which corresponds to the two-nucleon S -wave channel), the phase shift is attractive at low energy region while it becomes repulsive

as the energy increases. In the second case ($\nu = 2/9$, which corresponds to $\Sigma N(I=3/2, S=1)$), the phase shift is repulsive at low energy region while it becomes attractive as the energy increases. These behaviors of the phase shifts can be understood in the following way. Since the Pauli-blocking changes the degrees of the mixing between the incoming wave and the 0ℓ state of the inter-cluster wave function, the behavior of the resulting effect above the energy of the 0ℓ state is different from that in the lower energy-region.

We also look into the properties of this nonlocal potential by constructing four kinds of local potentials: 1) the one which gives the same scattering phase shift as

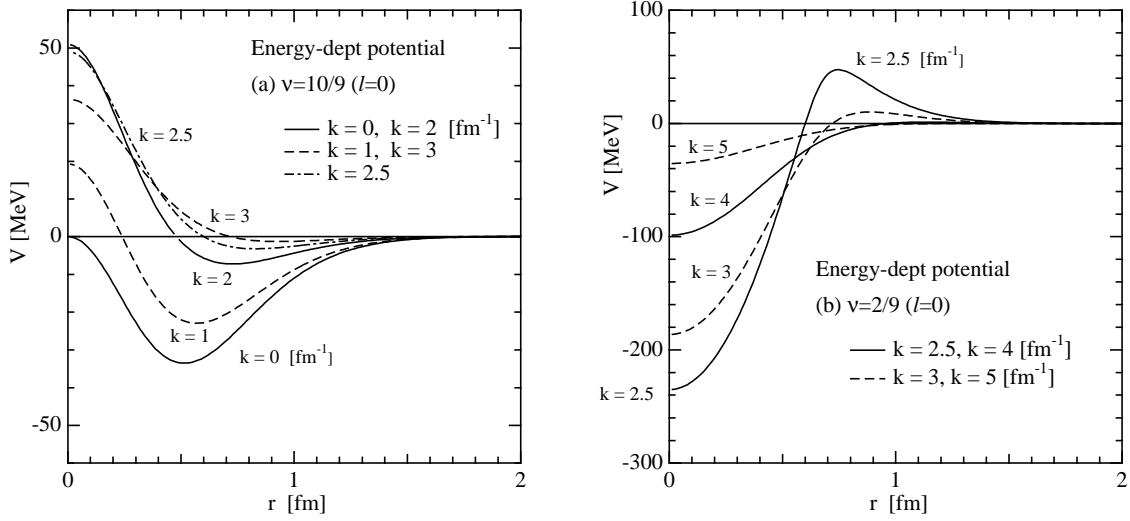


FIG. 11: Energy-dependent potentials with the WKB method, $U(r, E)$ (see text). (a) is for the $\nu = 10/9$ case. (b) is for the $\nu = 2/9$ case.

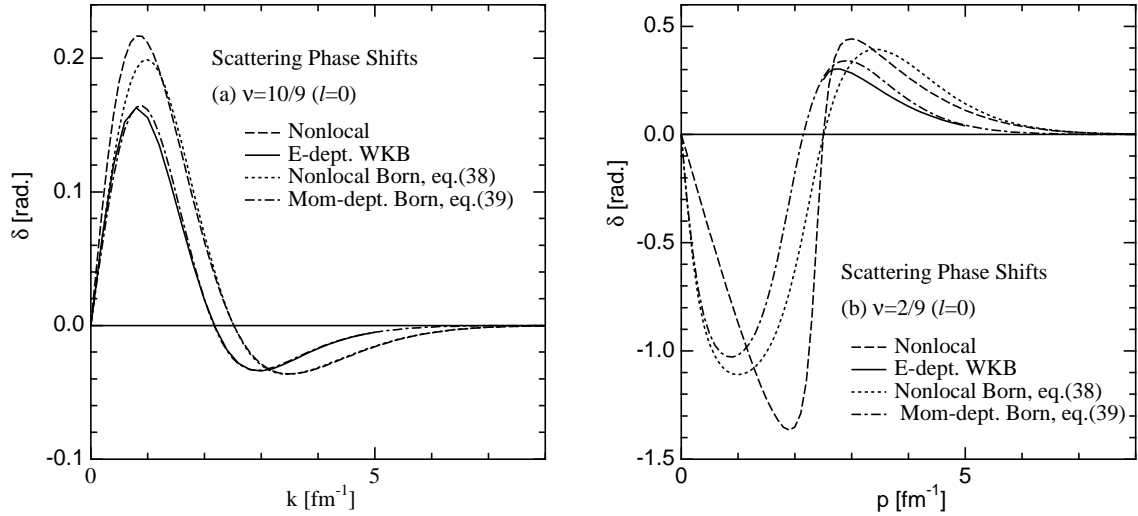


FIG. 12: Scattering phase shifts obtained from the energy-dependent potentials with the WKB method as well as those of the momentum-dependent potentials with the Born approximation. (a) is for the $\nu = 10/9$ case. (b) is for the $\nu = 2/9$ case, where that of the WKB method is calculated only above $k \geq 2.5 \text{ fm}^{-1}$.

that of the original potential, 2) the one which gives the same Born phase shift, 3) the one with energy dependent potentials obtained from the wave function, and 4) the one with energy dependent potentials obtained by the WKB method. It is found that the behavior of the equivalent local potentials depends strongly on the size of the Pauli-Blocking effect.

In the channel where the Pauli-blocking effect is small ($\nu = 10/9$), the former two local potentials, which are very similar to each other, simulate the nonlocal potential well even for the off-shell behavior. The energy dependent potentials given by the WKB method can also be

obtained and found to increase as the energy increases.

On the other hand, where the Pauli-blocking effect is large ($\nu = 2/9$), the off-shell behavior of the equivalent local potential is very different from the original one. It is because the local potential simulates the almost-forbidden resonance by having a deep attractive pocket at the very short range with a large barrier. Therefore it is very difficult to simulate the on- and off-shell behavior of the nonlocal potential simultaneously in terms of the local potential. However, if we keep the main part of the nonlocal potential, namely, the term coming from the $0s$ - $1s$ component, the rest terms can be

nicely simulated by a local potential not only for the on-shell but also for the off-shell behaviors. We have also calculated the energy-dependent potential by the WKB method and found that it becomes complex potential at some area. For the higher energy, the obtained potential is real. There we also find an attractive pocket and a barrier, both of which disappear as the energy increases.

The preset work indicates that in a certain channel the nonlocal treatment is essential. The place where the off-shell features become important, such as the baryons in nuclei, it should be checked whether the use of a local potential is appropriate or not. For this purpose, non-locality in the contribution from the interaction between quarks should also be considered. It is also interesting to see the situation in coupled-channel systems, which is now underway.

This work is supported in part by the JSPS Grant-in-Aid for Scientific Research (C)(2)11640258 and (C)(2)12640290.

appendix

Here we show how we expand the exchange term of the orbital normalization kernel, $N_{\text{ex}}(\mathbf{x}, \mathbf{y})$. This term has the form,

$$N_{\text{ex}}(\mathbf{x}, \mathbf{y}) = N_0 \exp[-S(x^2 + y^2) + 2T\mathbf{x} \cdot \mathbf{y}] , \quad (44)$$

which can be expanded as

$$N_0 \sum_{n\ell m} \theta^{2n+\ell} \psi_{n\ell m}(\beta, \mathbf{x})^* \psi_{n\ell m}(\beta, \mathbf{y}) \quad (45)$$

Here, $\psi_{n\ell m}(\beta, \mathbf{x})$ is the harmonic oscillator wave function with the size parameter β . N_0 , S and T in eq. (44) can be expressed by using β and θ , as

$$N_0 = \{\pi\beta^2(1-\theta^2)\}^{-3/2} \quad (46)$$

$$S = \frac{1+\theta^2}{1-\theta^2} \frac{1}{2\beta^2} \quad (47)$$

$$T = \frac{\theta}{1-\theta^2} \frac{1}{\beta^2} . \quad (48)$$

Suppose we have two clusters which consists of N_1 and N_2 particles exchanging n particles to each other. When the configuration of the clusters can be expressed as $(0s)^{N_1}$ and $(0s)^{N_2}$, respectively, with the size parameter b , we have

$$\beta^2 = \frac{N_1 + N_2}{N_1 N_2} b^2 \quad (49)$$

$$\theta = \frac{N_1 N_2 - n(N_1 + N_2)}{N_1 N_2} . \quad (50)$$

In the present study, $N_1 = N_2 = 3$ and $n = 1$. So, $\beta^2 = \frac{2}{3}b^2$ and $\theta = 1/3$.

The exchange part of the kinetic kernel can be written as

$$K_{\text{ex}}(\mathbf{x}, \mathbf{y}) = K_0 [-U(x^2 + y^2) + 2V\mathbf{x} \cdot \mathbf{y} + W] N_{\text{ex}}(\mathbf{x}, \mathbf{y}) \quad (51)$$

where

$$K_0 = \frac{3}{4mb^2} \quad (52)$$

$$U = \frac{1+3\theta^2}{(1-\theta^2)^2} \frac{2}{3\beta^2} \quad (53)$$

$$V = \frac{\theta(3+\theta^2)}{(1-\theta^2)^2} \frac{2}{3\beta^2} \quad (54)$$

$$W = \frac{5-\theta^2}{1-\theta^2} + N_1 + N_2 - 4 . \quad (55)$$

Or, it can be expanded as

$$K_{\text{ex}}(\mathbf{x}, \mathbf{y}) = (N_1 + N_2 - 2) K_0 N_{\text{ex}}(\mathbf{x}, \mathbf{y}) + \sum_{nn'\ell m} K^{nn'\ell} \psi_{n\ell m}(\beta, \mathbf{x}) \psi_{n'\ell m}^*(\beta, \mathbf{y}) \quad (56)$$

with

$$K^{nn'\ell} = \frac{2K_0}{3} \left\{ \delta_{nn'} \left(2n + \ell + \frac{3}{2} \right) + (\delta_{nn'+1} + \delta_{nn'-1}) \sqrt{(n_{<} + 1) \left(n_{<} + \ell + \frac{3}{2} \right)} \right\} \theta^{2n_{<} + \ell} \quad (57)$$

where $n_{<}$ corresponds to the smaller one between n and n' .

[1] Prog. Theor. Phys. Suppl. **62**(1977) and **68**(1980), edited by K. Ikeda.

[2] M. Oka and K. Yazaki, Phys. Lett. **B90**(1980)41;

- Prog. Theor. Phys. **66**(1981)556; Prog. Theor. Phys. **66**(1981)572.
- [3] A. Faessler, F. Fernandez, G. Lübeck and K. Shimizu, Phys. Lett. **B112**(1982)201; Nucl. Phys. **A402**(1983)555.
 - [4] M. Oka and K. Yazaki, Quarks and Nuclei, ed. W. Weise (World Scientific, Singapore, 1985).
 - [5] K. Shimizu, Rep. Prog. Phys. **52**(1989)1.
 - [6] Prog. Theor. Phys. Suppl. **137**(2000), edited by M. Oka, K. Shimizu and K. Yazaki.
 - [7] S. Takeuchi and K. Shimizu, Phys. Rev. **C 65** (2002)064006.
 - [8] S. Takeuchi and K. Shimizu, Phys. Lett. **B 179** (1986)197.
 - [9] Y. Fujiwara, *et. al.*, Phys. Rev. **C66**(2002)021001.
 - [10] S. Takeuchi, hep-ph/0008185.
 - [11] R.G. Newton, Scattering Theory of Waves and Particles (New York: Springer-Verlag, 1982).
 - [12] Z.S. Agranovich and V.A. Marchenko, The Inverse Problem of Scattering Theory (New York: Gordon and Breach, 1963).
 - [13] K. Chadan and P. C. Sabatier, Inverse Problems in Quantum Scattering Theory (2nd ed.) (New York: Springer-Verlag, 1989).
 - [14] Y. Suzuki and K.T. Hecht, Phys. Rev. **C27**(1983)299; **C28**(1983)1458.